Disruption of the Gene Encoding the β1-Subunit of Transducin in the *Rd4*/+ Mouse

Eiko Kitamura,[1] *Michael Danciger,*[2] *Clyde Yamashita,*[1] *Nagesh P. Rao,*[3] *Steven Nusinowitz,*[1] *Bo Chang,*[4] *and Debora B. Farber*[1,5]

Purpose. The *Rd4*/+ mouse inherits an autosomal dominant retinal degeneration that cosegregates with a large inversion spanning nearly all of mouse chromosome 4 (Chr 4). This inversion is homozygous lethal. The hypothesis for the study was that disruption of a gene at one of the two breakpoints in the *Rd4* chromosome is responsible for the retinal degeneration. The purpose was to identify the disrupted gene.

Methods. Genotyping was performed by PCR and gel electrophoresis. The *Rd4*/+ phenotype was confirmed by ERG. Fluorescence in situ hybridization (FISH) analysis was performed with bacterial artificial chromosome (BAC) probes. Northern and quantitative PCR procedures were used to evaluate *Gnb1* mRNA expression. Protein expression was measured by Western blot.

Results. To identify the *Rd4* gene defect, the breakpoints were first localized with a testcross and the locus refined by using FISH. Genetic testcross data revealed that the inversion breakpoints are located within a few centimorgans of both the telomeric and centromeric ends of Chr 4. Initial FISH analysis showed the proximal breakpoint of the inversion to be in the centromere itself. Therefore, we focused on the distal breakpoint and found that it lies in the second intron of the gene *Gnb1*, coding for the transducin β1-subunit (Tβ1) protein that is directly involved in the response to light of rod photoreceptors. Before the beginning of retinal degeneration in *Rd4*/+ retina, the levels of *Gnb1* mRNA and Tβ1 protein are 50% of those in wild-type retina.

Conclusions. The results suggest that disruption of the *Gnb1* gene is responsible for *Rd4* retinal disease. (*Invest Ophthalmol Vis Sci.* 2006;47:1293–1301) DOI:10.1167/iovs.05-1164

Retinal degeneration is a major cause of visual impairment and blindness in humans. In recent years, remarkable progress has been made in the identification of genes responsible for various forms of retinal degeneration, and, to date, more than 160 loci have been discovered. The defective gene has been identified in more than 110 of these loci (Retinal Information Network; www.sph.uth.tmc.edu/RetNet/home.htm, provided in the public domain by the University of Texas Houston Health Science Center, Houston, TX). Some of these genes were first identified in mouse models and then were found to be associated with human disorders. For example, the discovery that a mutant cGMP-phosphodiesterase β-subunit gene (*Pde6b*) was responsible for the *rd1* mouse retinal degeneration[1–3] led to the identification of mutations in the β-subunit of cGMP-phosphodiesterase in individuals affected with autosomal recessive retinitis pigmentosa.[4–6] Furthermore, finding the defective *rd7* gene[7] created the opportunity to study the molecular pathways that regulate normal retinal development and to understand some of the consequences of mutations in *NR2E3* that cause enhanced S-cone syndrome in humans.[8–10] The *Rd4*/+ degeneration was found in a stock carrying the chromosomal inversion In(4)56Rk, which was induced in a DBA/2J male[11] and bred onto the C57BL/6J background. As reported in this study, in the affected mouse, the photoreceptor layer of the retina had degenerated completely and the electrophysiological response to light (as measured by the electroretinogram [ERG]) had completely disappeared by 6 weeks of age. The phenotype is inherited in an autosomal dominant fashion and is always associated with an inversion encompassing nearly all of chromosome (Chr)4. Homozygous inheritance of the *Rd4* chromosome is lethal. In this article, we describe the identification of the gene disrupted at the distal breakpoint of Chr 4 in the *Rd4* mouse. Because our initial experiments demonstrated that the proximal breakpoint was in the centromere itself and that the distal breakpoint was in the subtelomeric region of Chr 4, we used FISH to first flank and then identify this distal breakpoint. Bacterial artificial chromosomes (BACs) that hybridized to the remaining, uninverted telomeric region and those that hybridized to the proximal inverted region of the chromosome were tested. Finally, a single BAC that hybridized to both ends of the chromosome was identified. We hypothesized that this BAC would contain the sequence harboring the breakpoint. Using FISH, we discovered that the breakpoint of the mutant Chr 4 is in the second intron of the *Gnb1* gene. This disruption decreases by ~50% the expression of both message and protein of the *Gnb1* gene in heterozygotes before the onset of retinal degeneration.

Methods

Animals

C57BL/6J (B6)+/+ and *Rd4*/+ mice were obtained from colonies bred from stock originated at the Jackson Laboratory (Bar Harbor, ME). Mice were reared under dim cyclic light and killed at appropriate postnatal days. The eyes were quickly enucleated after death and the retinas dissected rapidly and frozen on dry ice. All experiments were conducted in accordance with the Animal Care and Use Committee of UCLA and the ARVO Statement for the Use of Animals in Ophthalmic and Vision Research. For the backcross, stock *Rd4*/+ mice were bred to *Mus spretus* mice to produce F1 mice. The *Rd4*/+ F1 mice were distinguished from +/+F1 mice by fundus observation with an oph-

From the [1]Jules Stein Eye Institute, the [5]Molecular Biology Institute, and the [3]Department of Pathology, David Geffen School of Medicine at UCLA, Los Angeles, California; the [2]Biology Department, Loyola Marymount University, Los Angeles, California; and [4]The Jackson Laboratory, Bar Harbor, Maine.

Supported by a Post-Doctoral Fellowship from Fight for Sight (EK) and by the Foundation Fighting Blindness and National Eye Institute Grant EY08285 (DBF). DBF is a recipient of a Research to Prevent Blindness Senior Investigators Research Award.

Submitted for publication August 30, 2005; revised December 9, 2005; accepted February 24, 2006.

Disclosure: **E. Kitamura**, None; **M. Danciger**, None; **C. Yamashita**, None; **N. P. Rao**, None; **S. Nusinowitz**, None; **B. Chang**, None; **D.B. Farber**, None

The publication costs of this article were defrayed in part by page charge payment. This article must therefore be marked "*advertisement*" in accordance with 18 U.S.C. §1734 solely to indicate this fact.

Corresponding author: Debora B. Farber, Jules Stein Eye Institute, David Geffen School of Medicine at UCLA, Los Angeles, CA 90095; farber@jsei.ucla.edu.

Copyright © Association for Research in Vision and Ophthalmology

Downloaded from iovs.arvojournals.org on 08/16/2022

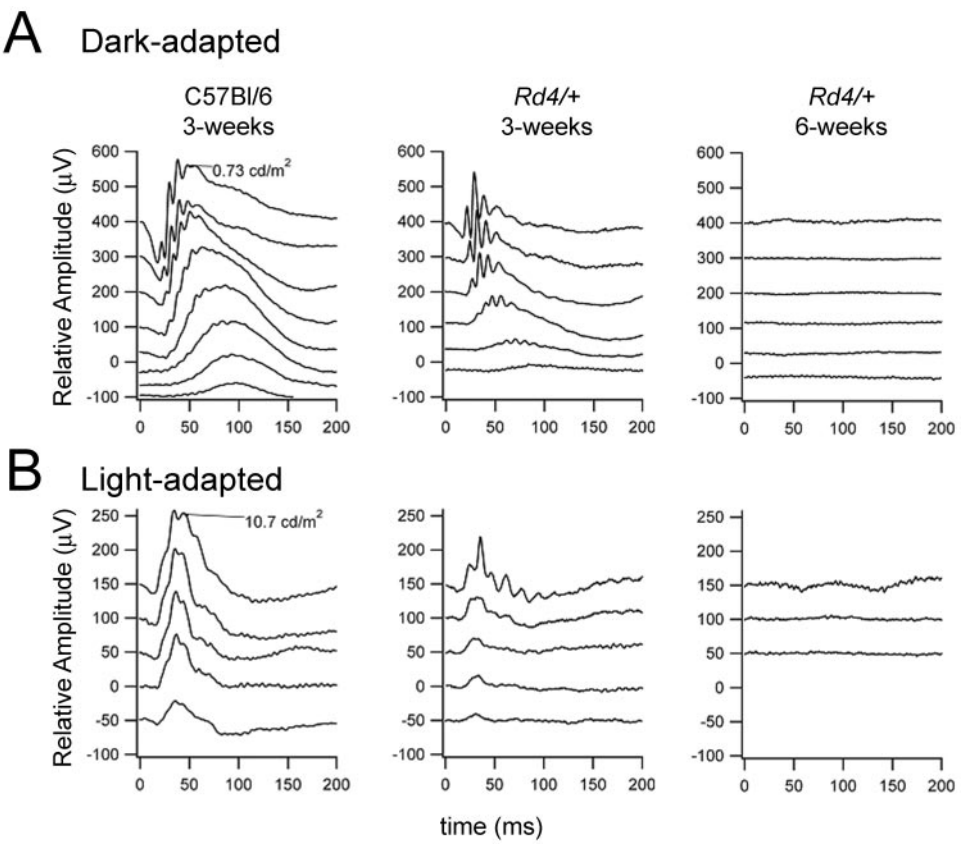

FIGURE 1. ERG recordings from a representative 3-week-old C57BL/6J mouse (*left*), and 3-and 6-week old *Rd4*/+ mice (*middle* and *right*, respectively). (**A**) Rod-mediated ERGs recorded to blue flashes of light of increasing intensity. (**B**) Cone-mediated ERGs recorded to white flashes of increasing intensity.

thalmoscope. *Rd4*/+ F1 mice were crossed to B6 mice and the 284 N2 progeny phenotyped for *Rd4* disease by fundus examination. The *Rd4*/+ phenotype was confirmed by ERG in a small cohort of these animals. ERG methodology has been described.[12] Figure 1 shows the typical results obtained for the rod and cone responses of *Rd4*/+ mice at 3 and 6 weeks of postnatal life.

Genotyping

After phenotyping, mice were killed, and DNA was isolated from liver tissue by standard procedures. Distal Chr 4 dinucleotide repeat markers polymorphic between the *M. spretus* and B6-*Rd4*/+ strains included *D4Mit180*, *D4Mit42*, *D4Mit357*, *D4Mit253*, *D4Mit344*, *D4Mit209*, and *D4Mit51.* Genotypes were determined by PCR and agarose gel electrophoresis.

Fluorescence In Situ Hybridization Analysis

Metaphase chromosomes were prepared from primary cultures of mouse ear-clips. Slides of metaphase chromosomes were made using standard cytogenetic procedures. Fluorescence in situ hybridization (FISH) analysis was performed basically as described.[13] BACs were obtained from Invitrogen (Chicago, IL). Total BAC DNA was labeled with digoxigenin-11-dUTP (DIG-Nick Translation Mix; Roche Molecular Biochemicals, Indianapolis, IN) or biotin (Bio Nick Labeling System; Invitrogen). Signals were detected with anti DIG-FITC (Roche Molecular Biochemicals) or Texas red avidin (ID Laboratories Inc., London, Ontario, Canada).

When small DNA fragments were used for FISH, several PCR products (0.5–1.0 kb) were combined and used as probes. Each mixture of PCR products covered approximately 2.0 kb of the genomic region. Primer sequences are shown in Table 1. The probe was labeled with a DNA labeling system (Bio Prime; Invitrogen). Because small DNA fragments give a very low intensity signal, we amplified the signals by incubating the slides with 1:500 diluted FITC avidin D (Vector Laboratories Inc., Burlingame, CA) and then hybridizing them with 1:100 diluted biotinylated goat anti-avidin D (Vector Laboratories Inc.). Signals were detected by incubating again with 1:500 diluted FITC avidin D. The chromosomes were counterstained with 4′,6′-diamino-2-phenylindole (DAPI) and viewed on a microscope (Axiophot; Carl Zeiss Meditec, Inc., Dublin CA) equipped with appropriate filters and a charge-coupled device (CCD) camera for image analyses.

TABLE 1. Primers Used to Prepare Probes for FISH Analysis

Probe	Primer	5′–3′
11-1	Forward-1	TTC CTG CTT CTC TGG TTT CC
	Reverse-1	GGG CTC CAC AAA GAC TCA TC
	Forward-2	CCC CGT GGG TAC TCT GTC T
	Reverse-2	AGC TTA GGA CCC CTT TCC AC
11-2	Forward-1	AGC CCT GAC AAT TAG CTC CA
	Reverse-1	CTT GCT GCC CAC TCT TTC TC
	Forward-2	TTG GAT TTT CAG TCA GGA ATC A
	Reverse-2	TCC TCA AAA CGA GCA AAA GG
11–3	Forward-1	TCT GAG TTG TTC TTT CTG TGC TG
	Reverse-1	GCT TAG TGA GAC GCT CAA GGA
	Forward-2	TTG TGT GTG GAT AAC AGA GTG AGA
	Reverse-2	TCT GCT CTC TAT GGT GGC CTA
	Forward-3	GCA CCA CCT CTA TTG GCA TT
	Reverse-3	TCT CAC TCT GTT ATC CAC ACA CAA
11–4	Forward-1	GAT GAG CCT CCT GCT TTG TC
	Reverse-1	CGA TTC AAG GTT GGA ATG GT
	Forward-2	TGA TCC TGT TCT GTG GCA TT
	Reverse-2	GTG GAC AGT GAG GGG ACA G
	Forward-3	CTG GAA GAA CAG CCT TTT GC
	Reverse-3	CAT CAC ACC AGA GTC CCT CA

Downloaded from iovs.arvojournals.org on 08/16/2022

TABLE 2. Primers Used for Real-Time Quantitative RT-PCR

Gene	Primer	5′–3′
Gnb1	Forward	TGA TGC TTC AGC CAA GCT CT
	Reverse	ACC TGC TCT GTC AGC TTT GA
Gnat1	Forward	GAC GAC GAA GTG AAC CGA AT
	Reverse	GGT GAC AGC GTC AAA GAC AA
Rho	Forward	TCG TCA TCT TCT TCT GCT ATG G
	Reverse	AGC GTG GTG AGC ATA CAG TT
BC004012	Forward	TCT GCA CTT TCC GTG AAG AC
	Reverse	ATT TTC ACT GAG GCC GTT GT
NM-177186	Forward	TGG ATA TCC CTG TGA TTG GAA
	Reverse	TGT GTC ATC TTC TGG GTT TCG
Cdc211	Forward	AAT GGC GAG AGA ACA TTC CA
	Reverse	TGT CTT GGA GGT CTG ACA ACA
Mmp23	Forward	GGC AGC TCA GGG AAA TGT AG
	Reverse	GGT TTG TGA GCC AAA CAC CT
NM-145124	Forward	CGC GTC TGC TTT GAC TAT GA
	Reverse	ACA CGT TCG TGG TTC CAT CT

Northern Hybridization

The cDNA clones used in this study were obtained from our mouse retinal libraries or prepared by RT-PCR using RNA from C57BL/6J retina. Total RNA was extracted from retinas of *Rd4*/+ and C57BL/6 mice (RNAzol B; Teltest, Inc., Friendswood, CA; or NucleoSpin RNA and Virus Purification Kits; BD-Clontech, Palo Alto, CA). Extracted RNA was separated by electrophoresis in 1.0% agarose gels containing 2.2 M formaldehyde, and transferred to Hybond-N^+ membranes (GE Healthcare, Piscataway, NJ). cDNA probes were labeled with [α-^{32}P]dCTP using the Rediprime II Random Prime Labeling System (GE Healthcare). After hybridization overnight in 0.25 M phosphate buffer, 1 mM EDTA, 7% SDS, and 1% bovine serum albumin at 65°C, the Northern blots were washed at a final stringency of 0.1× SSC, 0.1% SDS at 65°C and then exposed to x-ray film (GE Healthcare) for 2 to 16 hours at −80°C. The intensity of the signals was measured (ChemiImager 5500; Alpha Innotech Corp., San Leandro, CA).

Real-Time Quantitative RT-PCR

The expression of mRNAs in C57BL/6J and *Rd4*/+ retinas was analyzed by real-time quantitative RT-PCR. Total RNA was isolated from C57BL/6J and *Rd4*/+ mouse retinas, as described earlier, and then treated with Turbo DNA-free (Ambion, Austin, TX) to remove the contaminating genomic DNA. Single-stranded cDNA was synthesized with reverse transcriptase (Improm-II; Promega, Madison, WI) and oligo(dT) primers. The resultant cDNA was amplified on the Mx3000 instrument (Stratagene, La Jolla, CA) using Brilliant SYBR Green QPCR master mix, which contains SureStart *Taq* DNA polymerase, SYBR Green-I dye, dNTPs, and the reference dye (Stratagene). The PCR reaction was run under the following conditions: denaturation at 95°C 10 minutes, followed by 40 cycles of 95°C for 30 seconds, 60°C for 1 minute, and 72°C for 30 seconds. Amplified products were incubated at 95°C for 1 minute and 55°C for 30 seconds to plot dissociation curves. Primers were chosen from exons separated by large introns, and the PCR quality and specificity was verified by dissociation curve analysis and gel electrophoresis of the amplified products. The primer sets used are shown in Table 2.

Western Blot Analysis

Retinal homogenates were centrifuged at 1000*g* for 5 minutes. Proteins in the supernatants were separated by SDS-PAGE on a 12.5% T/3.0% C gel,[14] using a Tris/glycine buffer. They were blotted to a polyvinylidene difluoride (PVDF) membrane and incubated with a 1:4000 dilution of a Tβ1 antiserum (PA1-725, an antibody against a peptide corresponding to residues 8-25 of the Tβ1 sequence). Bands were visualized using alkaline phosphatase coupled to anti-rabbit secondary antibody and a chemiluminescence system (ECL; GE Healthcare).

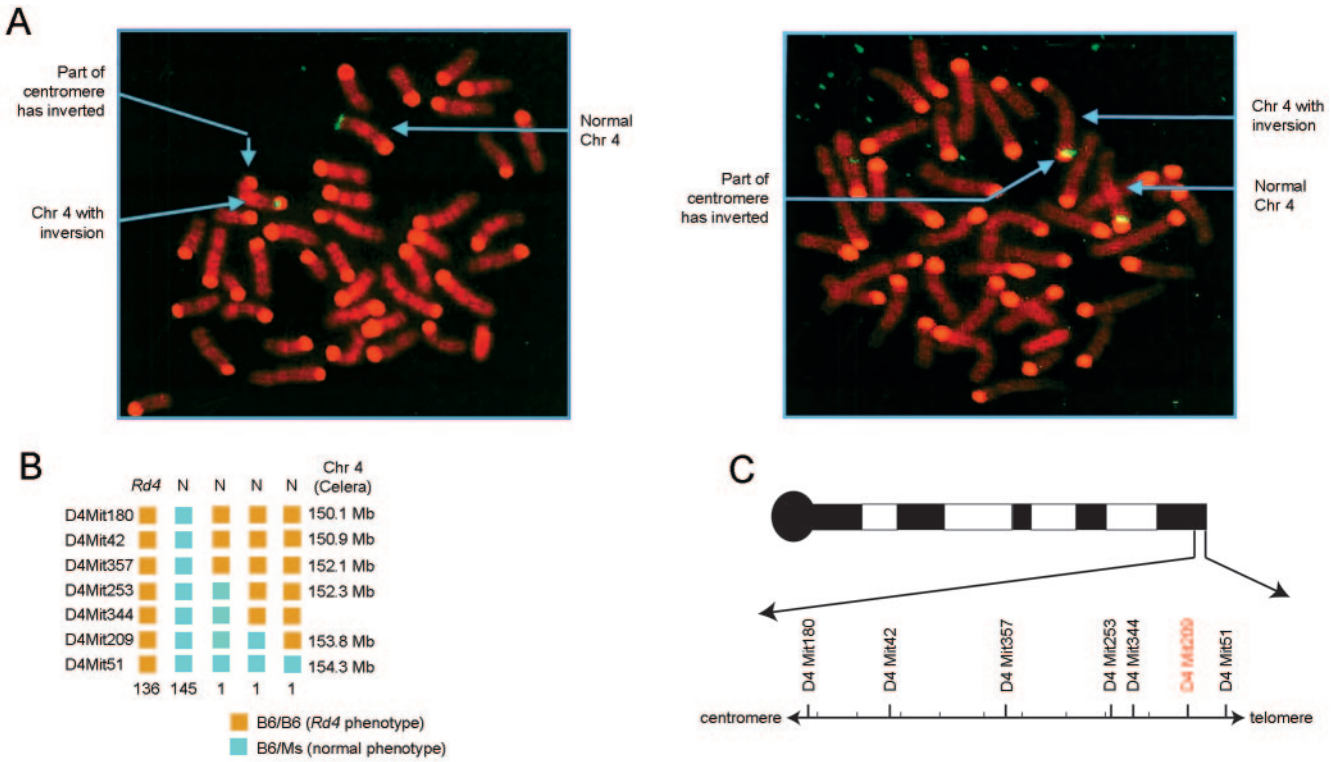

FIGURE 2. Genetic localization of the distal breakpoint of the *Rd4* chromosome. (**A**) FISH analysis of chromosomes from *Rd4*/+ mouse probed with a distal (*left*) and a proximal (*right*) BAC. (**B**) Alleles of the N2 progeny of the backcross [*Rd4*/+(B6) x *M. Spretus* (Ms)]F1 x B6. *Gold boxes*: homozygous C57Bl/6J; *cyan boxes*: C57Bl/6J/Ms. N, normal phenotype; *Rd4*, affected phenotype. (**C**) Physical map of the subtelomeric region of Chr 4. The breakpoint is distal to *D4Mit209*.

Downloaded from iovs.arvojournals.org on 08/16/2022

Sequence Analysis

The databases used for sequence analysis, BLAST and Map Viewer, can be found on the National Center for Biotechnology Information (NCBI) Web site (http://www.ncbi.nlm.nih.gov). The Primer 3 program was used to design primers (http://frodo.wi.mit.edu/cgi-bin/primer3/primer3-www.cgi, provided in the public domain by the Whitehead Institute, Massachusetts Institute of Technology, Cambridge, MA).

Results

At the outset of the study, we hypothesized that a gene disrupted at one of the inversion breakpoints was responsible for retinal disease in the *Rd4*/+ mouse. Initially, we performed FISH studies and determined that the proximal breakpoint of the inversion on Chr 4 was in the centromere (Fig. 2A). Therefore, since protein-expressing genes are unlikely to be centromeric, we focused our studies on the distal breakpoint.

Genetic Approximation of the Distal Breakpoint

To determine the general region of the distal breakpoint, we conducted the backcross [*Rd4*/+ (B6) x *Mus spretus* (Ms)]F1 x B6. The progeny of this cross that were *Rd4*/+ should have been homozygous B6 and those that were +/+, heterozygous B6/Ms. Any mice not fitting these categories would be recombinants. It should be noted that because of the inversion, single recombinant *Rd4* chromosomes would have either two centromeres or no centromeres; both formations are nonviable. Therefore, the only viable recombinants were rare double

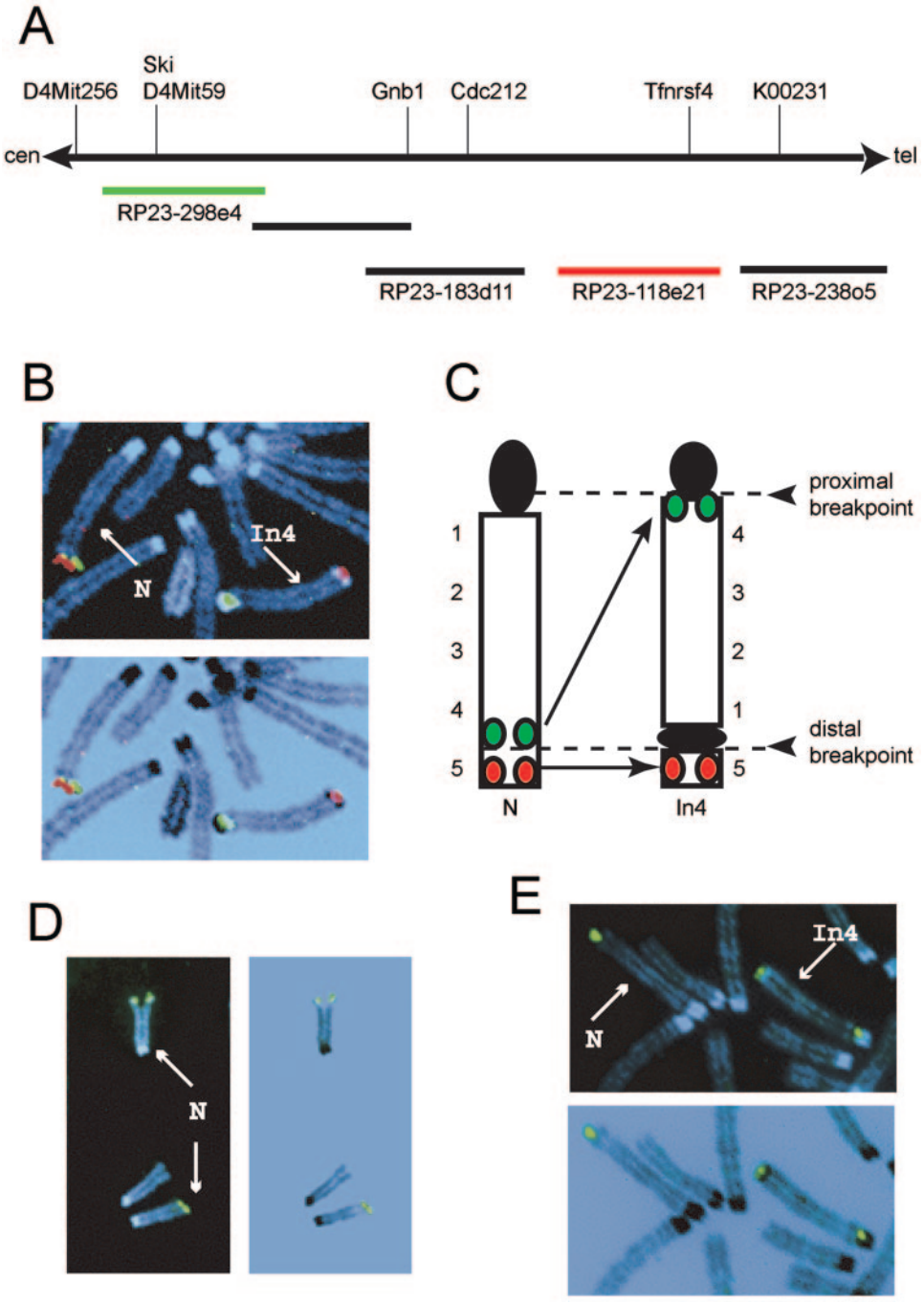

Figure 3. Characterization of the distal breakpoint region. (**A**) Physical map of the critical region for *Rd4* (not in scale). Markers are indicated *above* the diagram. BAC clones are shown as *solid bars* with RP23 addresses. (**B**) *Top*: dual-color FISH was performed with BAC clones, RP23-298e4 (*green*) and RP23-118e21 (*red*). *Bottom*: The FISH image was processed to show the split centromeres (dark-stained regions), which allow identification of the *Rd4* allele. (**C**) The ideogram with the expected localization of the signals obtained using RP23-298e4 (*green*) and RP23-118e21 (*red*). (**D**) BAC clone RP23-183d11 labeled with FITC was hybridized to a chromosome spread prepared from a normal C57BL/6J mouse. (**E**) Hybridization with RP23-183d11 to a chromosome spread from a *Rd4*/+ mouse demonstrates split signals on *Rd4* allele. N, normal allele; In4, inverted allele.

Downloaded from iovs.arvojournals.org on 08/16/2022

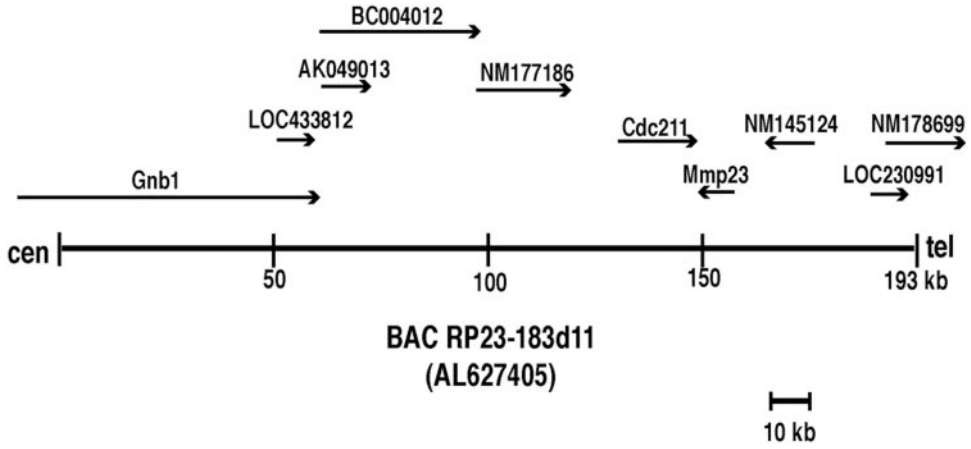

FIGURE 4. Genes and cDNA clones mapped on the BAC RP23-183d11, which spans the region of the distal breakpoint. *Arrows*: orientation of each gene.

recombinants. The 284 mouse progeny were phenotyped by fundus examination and genotyped with a set of seven distal Chr 4 dinucleotide repeat markers (see the Methods section). Only three recombinants were found (Fig. 2B), and each had a normal fundus but was homozygous B6 for some of the markers. The most informative progeny mouse had a normal fundus but was homozygous B6 at *D4Mit209* and heterozygous at *D4Mit51*. This placed the breakpoint distal to *D4Mit209* (Fig. 2C).

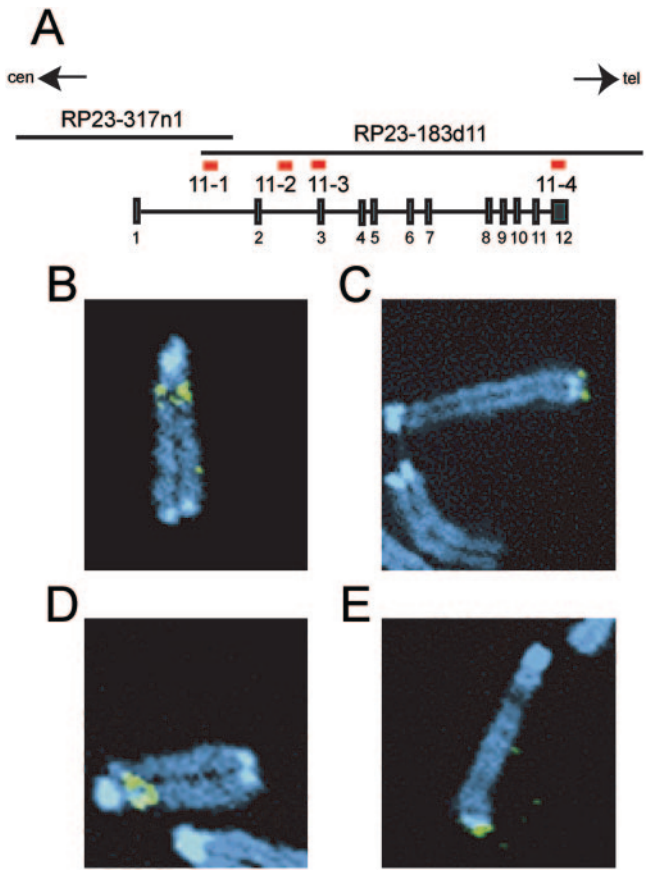

FIGURE 5. Localization by FISH of the distal breakpoint, using small genomic DNA fragments. (**A**) *Top horizontal lines*: BAC clones with RP23 addresses. *Bottom line with vertical boxes*: genomic structure of *Gnb1*. *Red bars*: small genomic fragments used as probes in FISH experiments. Fragments 11-1 and 11-2 are proximal to the breakpoint, because they hybridize to an inverted chromosomal region (**B**, **D**). Fragments 11-3 and 11-4 are distal to the breakpoint, because they hybridize to chromosomal regions that do not invert (**C**, **E**). The breakpoint region was narrowed down to the 10-kb region between fragments 11-2 and 11-3.

Identification of the Distal Breakpoint-Spanning BAC Clone

Using the NCBI Blast function (www.ncbi.nlm.nih.gov/genome/seq/MmBlast) we determined that *D4Mit209* is situated at 152.302 Mb and that Chr 4 ends at 154.141 Mb. Therefore, we had less than 2 Mb to work with. FISH experiments using several BAC clones distal to *D4Mit209* revealed that the critical region for *Rd4* is distal to the BAC RP23-298e4 (Fig. 3A). With this BAC as a starting point, we conducted several FISH experiments with additional BACs from a physical map of subtelomeric Chr 4 delineated by Li et al.[15] (Fig. 3A). Dual-color FISH was performed using the BAC clones, RP23-298e4 and RP23-118e21, labeled with digoxigenin (green) and biotin (red), respectively (Fig. 3B). For the normal Chr 4, both signals were localized on the telomeric end and the red signal of RP23-118e21 was immediately below the green signal of RP23-298e4 (Fig. 3B, top panel). This result corresponded to the physical order of these BAC clones (Fig. 3A). For the *Rd4* chromosome, the signal was split. Both BACs hybridized near the dark-

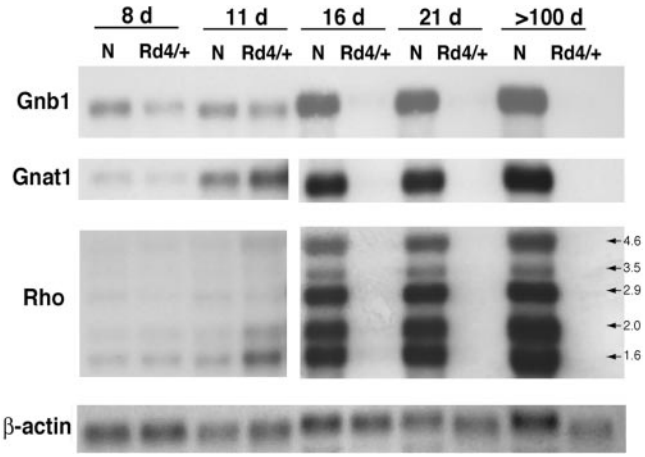

FIGURE 6. Expression of *Gnb1*, *Gnat1*, and *Rho* mRNAs during retinal development. Shown is a Northern blot of retinal RNA isolated at various ages of postnatal development. All lanes contain 5 μg of total RNA. β-Actin was used to normalize for RNA quantity per lane. Note that at P11 there was more RNA from *Rd4*/+ loaded than from C57BL/6J, as shown by the intensity of the β-actin signal of the same samples.

Downloaded from iovs.arvojournals.org on 08/16/2022

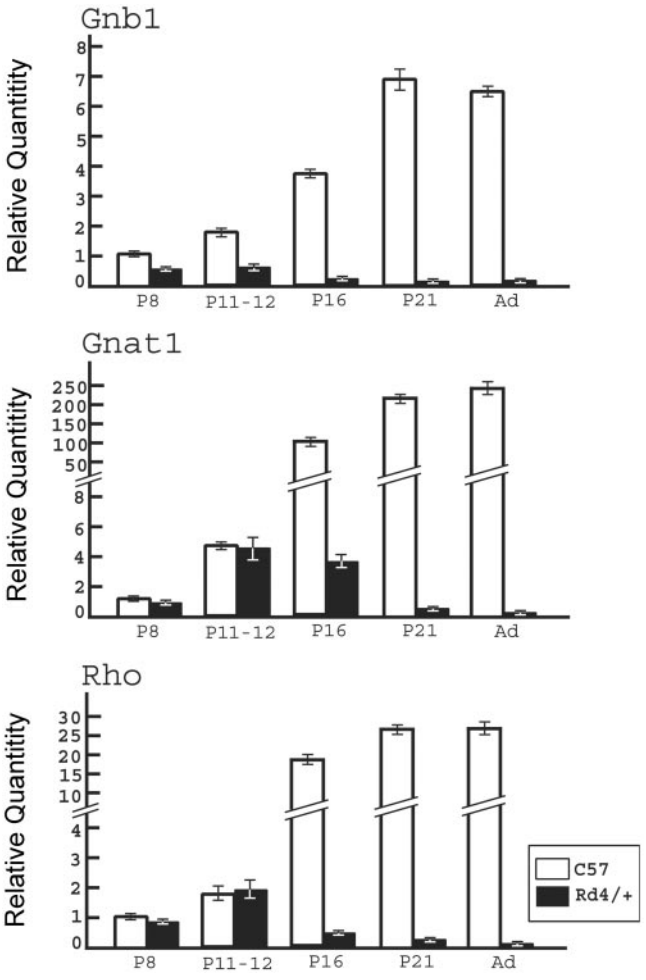

FIGURE 7. Expression levels of *Gnb1*, *Gnat1*, and *Rho* mRNAs at various postnatal ages determined by quantitative RT-PCR. mRNA expression was quantified relative to the expression of the corresponding gene in C57BL/6J at P8. The expression value was calculated as the mean of three independent quantitative RT-PCR experiments performed in duplicate. Error bars, ±SEM. For the *Rho* gene, only two transcripts (2.9 and 3.5 kb) were detected by the primer pair used.

staining (by DAPI) regions representative of centromeric DNA (Fig. 3B), but at opposite ends (the dark-staining regions are derived from the split centromere; Fig. 3B, bottom). The characteristic small and large centromere fragments were distinguished with the bright-field microscope. The green-stained RP23-298e4 hybridized immediately adjacent to the large centromere fragment and the red-stained RP23-118e21 hybridized near to the small centromere fragment (Fig. 3B). Therefore, the distal breakpoint had to be between these two BAC clones, with green RP23-298e4 proximal to the breakpoint (inverted) and red RP23-118e21 distal (not inverted; Fig. 3C). With further analysis, we found that the single BAC RP23-183d11 (Fig. 3A) gave a split signal on the *Rd4* Chr 4 (Fig. 3E) and a telomeric signal on the normal Chr 4 (Figs. 3D, 3E). This indicated that the distal breakpoint was within the chromosomal region complementary to RP23-183d11.

Delineation of the Position of the Telomeric Breakpoint

A total of 193 kb of sequence of RP23-183d11 (AL627405) has been completed and is available from the NCBI database. Analysis of this complete sequence using the NCBI BLAST server and NCBI Map Viewer revealed the presence of three known genes (*Gnb1*, *Cdc211*, and *Mmp23*), four unknown genes (*BC004012*, *NM-177186*, *NM-145124*, and *NM-178699*), one unknown expressed sequence tag (EST; AK049013), and two predicted genes (*LOC433812*, *LOC230991*) within this BAC clone (Fig. 4).

To identify which gene was disrupted by the distal breakpoint, genomic DNA fragments of RP23-183d11 were prepared by PCR amplification and used as probes for FISH (Fig. 5A). Primer sequences are listed in Table 1. A minimum of 20 metaphases was analyzed for each FISH study. Probe 11-1 hybridized below the large centromere region of the *Rd4* chromosome (Fig. 5B) and probe 11-4 below the small centromere region (Fig. 5C), indicating that the breakpoint was in the interval between them. Only one known gene, *Gnb1* has been mapped in this region and is oriented centromere to telomere (Fig. 4). After using several probes (data not shown), we found that probe 11-2 hybridized below the large centromere region and 11-3 below the small centromere region (Figs. 5D, 5E). Probe 11-2 contains sequence entirely from proximal intron 2 while probe 11-3 contains sequence starting in distal intron 2

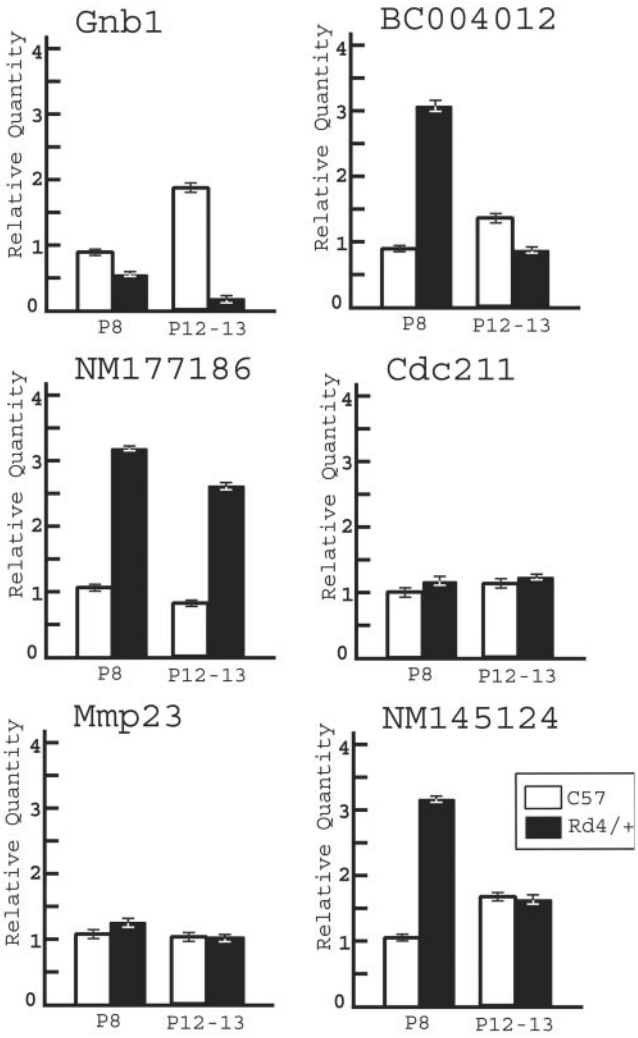

FIGURE 8. Comparative expression of genes mapped on the BAC RP23-183d11 at P8 and P12 to P13. mRNA expression was quantified relative to the expression of the corresponding gene in C57BL/6J at P8. The mRNA levels were calculated as the mean of three independent quantitative RT-PCR experiments performed in duplicate. Error bars, ±SEM.

Downloaded from iovs.arvojournals.org on 08/16/2022

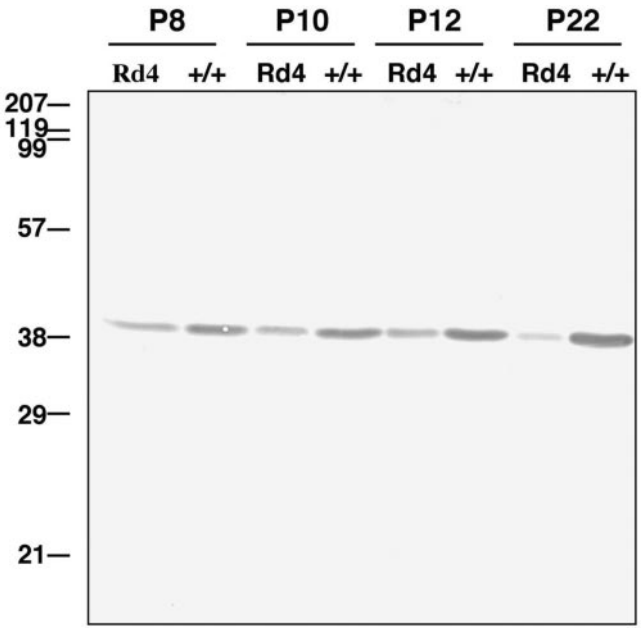

FIGURE 9. Comparison of transducin β1-subunit expression in *Rd4*/+ and C57BL/6J retinas. Each lane of the Western blot contains 25 μg protein. A polyclonal antibody specific for Tβ1-subunit was used at a 1:4000 dilution.

and extending into exon 3 of the *Gnb1* gene. This localized the breakpoint to intron 2.

To identify the breakpoint further, we performed Southern blot analysis, using restriction enzymes such as *Mae*III, *Pst*I, *Mbo*II, *Acc*I, and *Hin*cII, which are known to digest mouse satellite sequences frequently. Probes derived from intron 2 sequence were used for this experiment. We always detected fragments from normal chromosome 4 but not from *Rd4* chromosome 4. In the *Rd4* chromosome, intron 2 fragments must be attached to the split distal and proximal centromere fragments and, therefore, unable to migrate in the gel. In addition, sequencing of these areas near the centromere is difficult because they are organized into large blocks of highly repetitive satellite-DNA.[16] Several groups have reported sequences of mouse satellites[17–19] yet whole centromere sequences have not been fully characterized because of these repetitive blocks.

Developmental Expression Pattern of mRNA

Gnb1 spans at least 50 kb of genomic DNA and consists of 12 exons and 11 introns. The coding sequence starts in exon 3.[20] Our FISH results showed that in the *Rd4*/+ mouse the breakpoint is located in intron 2 of *Gnb1*. Therefore, its 5′-untranslated region (UTR) is interrupted and separated from the rest of the gene. Because of this interruption/separation, we hypothesized that expression of the *Rd4 Gnb1* allele would be completely shut down. To test this, the developmental expression patterns of *Gnb1* and other retina-specific mRNAs were measured by Northern blot analysis in normal and *Rd4*/+ retinas. There were no evident differences in expression levels of *Gnat1* and *Rho* mRNAs between *Rd4*/+ and C57BL/6J retinas at postnatal day (P)8 and P11 (Fig. 6). However, from P16, mRNAs for these two genes drastically decreased in *Rd4*/+ retinas, correlating with the photoreceptor loss that characterizes the *Rd4*/+ retina at this postnatal age.[11] In contrast, expression of *Gnb1* mRNA in *Rd4*/+ relative to C57BL/6J control retinas was reduced by approximately 50% at P8 and P11 (Fig. 6), suggesting haploinsufficiency due to the absence of expression of the *Rd4 Gnb1* allele, but normal expression from the normal *Gnb1* allele. These results were confirmed by real-time quantitative RT-PCR. The results show that the expression level of *Gnb1* mRNA in *Rd4*/+ retina is 58% of wild-type at P8, and 36% at P11 (Fig. 7, top). For the *Gnat1* and *Rho* transcripts, there is no significant difference in expression at P8 (Fig. 7, middle and bottom, respectively). Because the *Rho* primer pair used for real-time quantitative RT-PCR detects two transcripts (2.9 and 3.5 kb) of five, the relative quantity of *Rho* gene measured in adult retinas in these experiments is only 20- to 25-fold that obtained at P8. To examine for the possible presence of transcripts fused with the inverted *Gnb1* promoter-exon 1 and 2 sequence, we used a cDNA probe comprised of exons 1 to 7 for Northern blot analysis. No other transcripts were observed from *Rd4*/+ retina after a 5-day exposure to x-ray film (data not shown).

Comparison of mRNA Expression of Genes Mapped to the RP23-183d11 BAC

To examine whether genes that are close to the distal breakpoint are affected in their expression, we compared the mRNA level of five of such genes, *BC004012*, *NM177186*, *Cdc211*, *Mmp23*, and *NM145124* (see Fig. 4) using real-time quantitative RT-PCR and RNA from C57BL/6J and *Rd4*/+ retinas at two postnatal ages: P8 and P12 to 13 (Fig. 8). The expression pattern of *Gnb1* was consistent with that observed in Figure 6. For all five genes tested, the levels of mRNA were not lower in the *Rd4* mouse at P8 and P12 to P13 compared with those in the normal mouse. In fact, for three of the genes, *BC004012*, *NM177186*, and *NM145124*, the mRNA levels were clearly higher in *Rd4*/+ than in normal mice at P8 and then decreased at P12 to P13, correlating with photoreceptor cell death. No significant difference was detected in the other two genes, *Cdc211* and *Mmp23* between *Rd4*/+ and C57BL/6J at either age. These results show that the *Gnb1* expression pattern is completely different from that of these nearby genes, indicating that the presence of the distal breakpoint does not bring about any deleterious changes in their expression.

Expression of Tβ1 Protein

Levels of Tβ1 protein were analyzed by Western blot. Tβ1 protein was expressed at a lower level in *Rd4*/+ retina than in C57BL/6J retina at P8, P10, and P12 and continued to decrease with age (Fig. 9), consistent with the *Gnb1* mRNA expression pattern.

DISCUSSION

In this study, we have demonstrated that the distal breakpoint of the inverted *Rd4* Chr 4 is localized in the second intron of the *Gnb1* gene, whereas the proximal breakpoint lies within the centromere. The centromere plays an important role in the proper segregation of chromosomes during cell division. However, several investigators have found that centromere breaks and disrupted centromeres are stable in normal human samples both in mitosis and in meiosis, suggesting that these breaks neither impair the centromeric function nor have clinical effects.[21–23] Hence, the centromere DNA disruption observed in the *Rd4* chromosome probably does not contribute, in this case, to the observed retinal degeneration.

In addition, we have shown that the disruption of the *Gnb1* gene by the distal breakpoint reduces mRNA and protein expression in *Rd4*/+ retina. This is not surprising, because the gene is disrupted in intron 2, before the coding region that starts in exon 3, and transcription would result in a very small mRNA fragment that would not be translated. Therefore, no protein would be made from the disrupted allele. This finding, along with the fact that *Gnb1* encodes the transducin β1-

Downloaded from iovs.arvojournals.org on 08/16/2022

subunit, a protein involved in phototransduction and in the normal maintenance of photoreceptors, makes this disrupted gene the most likely cause of *Rd4* retinal degeneration. The locus of the *Rd4* breakpoint in the *Gnb1* gene at distal mouse Chr 4 is homologous to human chromosome 1, region p36, where *GNB1* maps. Recently, a locus for Leber's congenital amaurosis (LCA9; OMIM 608553; Online Mendelian Inheritance in Man; http://www.ncbi.nlm.nih.gov/Omim/ provided in the public domain by the NCBI, Bethesda, MD) has been identified between markers *D1S1612* and *D1S228* on 1p36.[24] The phenotype of LCA, which is characterized by severe retinal degeneration at birth or early onset, is similar to that of the *Rd4* mouse. LCA, however, is recessively inherited, whereas *Rd4* is inherited dominantly. In addition, a contig map from the NCBI database reveals that human *Gnb1* maps approximately 6.1 Mb distal to the LCA locus. Therefore, *Gnb1* is not a candidate gene for LCA9.

Several investigators have reported that translocation breakpoints are found to map outside the putative gene and that the gene defect is caused by a position effect of the breakpoint.[25] For example, *PAX6* haploinsufficiency at human chromosome 11, region q13, has been shown to cause aniridia, which is a congenital malformation characterized by severe hypoplasia of the iris. In two patients with aniridia, the translocation breakpoints mapped at 100 and 125 kb downstream of *PAX6*.[25,26] We investigated the possibility that the distal breakpoint provides a position effect on five other genes present in the BAC that includes the *Rd4* gene. We showed that the mRNA expression patterns of these genes are different from that of *Gnb1*. None showed decreased expression at P8 and P11 like *Gnb1*. These results indicate that there is no position effect of the distal breakpoint, at least on these five genes.

Gnat1$^{-/-}$ mice show a mild retinal degeneration, having a slightly thinner ONL (the outer nuclear layer of the retina; the nuclei of the photoreceptor rods and cones) compared with wild-type at 4 weeks of age and a thinner photoreceptor layer with one row of nuclei in the ONL at 13 weeks (normal is 10–12 rows of nuclei).[27] *Gnat1*$^{-/-}$ retina expresses the Tβ1 protein at a level that is close to normal. In *Gnat1*$^{-/+}$ mice, there is a small reduction of Tα protein content but retinal morphology is almost normal. Other groups have constructed *Rho*$^{-/-}$ mice[28,29] and have shown that at P15 *Rho*$^{-/-}$ retinas contain a normal number of nuclei in the ONL and normal-appearing inner segments, but that outer segments are absent. Although the ONL and inner segments become thinner with age, there is still one row of nuclei at P90. *Rho*$^{-/+}$ mice have shorter outer segments than normal in early life, but no significant degeneration is observed with age in these retinas. In contrast to these knockout mice, the *Rd4*/+ mouse has a severe, progressive, retinal degeneration that begins at P10 and results in complete loss of photoreceptor cells by 6 weeks of age.[11] In *Rd4*/+ retina, expression of *Gnb1* mRNA is reduced to ~50% that of control retina at an early stage, P8, whereas no obvious reductions of *Gnat1* and *Rho* mRNAs are detected at the same age. The complete absence of Tα in the *Gnat*$^{-/-}$ mouse causes only a mild retinal degeneration, whereas there is a severe phenotype associated with heterozygosity in the *Rd4*/+ mouse. This suggests that *Gnb1* may be essential not only for phototransduction but also for survival of photoreceptor cells. For example, the decreased levels of Tβ may impair the trafficking of other proteins or protein complexes contributing to the demise of the visual cells. Therefore, the association of a defective *Gnb1* gene with *Rd4* disease opens two avenues of study. The first, of course, is to screen patients with retinal degeneration for mutations in the human *GNB1* gene, and the second is to use the *Rd4* mouse to study the role that Tβ1 plays in the maintenance of photoreceptors.

Acknowledgments

The authors thank Elika Decker and Cathy Do for technical assistance.

References

1. Bowes C, Li T, Danciger M, Baxter LC, Applebury ML, Farber DB. Retinal degeneration in the *rd* mouse is caused by a defect in the β subunit of rod cGMP-phosphodiesterase. *Nature*. 1990;347:677–680.
2. Bowes C, Li T, Frankel WN, et al. Localization of a retroviral element within the *rd* gene coding for the β subunit of cGMP-phosphodiesterase. *Proc Natl Acad Sci USA*. 1993;90:2955–2959.
3. Pittler SJ, Baehr W. Identification of a nonsense mutation in the rod photoreceptor cGMP phosphodiesterase β subunit gene of the *rd* mouse. *Proc Natl Acad Sci USA*. 1991;88:8322–8326.
4. McLaughlin ME, Sandberg MA, Berson EL, Dryja TP. Recessive mutations in the gene encoding the β-subunit of rod phosphodiesterase in patients with retinitis pigmentosa. *Nat Genet*. 1993;4:130–134.
5. Danciger M, Blaney J, Gao Y, et al. Mutations in the PDE6B gene in autosomal recessive retinitis pigmentosa. *Genomics*. 1995;30:1–7.
6. Bayes M, Giordano M, Balcells S, et al. Homozygous tandem duplication within the gene encoding the β-subunit of rod phosphodiesterase as a cause of autosomal recessive retinitis pigmentosa. *Hum Mutat*. 1995;5:228–234.
7. Akhmedov NB, Piriev NI, Chang B, et al. A deletion in a photoreceptor-specific nuclear receptor mRNA causes retinal degeneration in the *rd*7 mouse. *Proc Natl Acad Sci USA*. 2000;97:5551–5556.
8. Haider NB, Jacobson SG, Cideciyan AV, et al. Mutation of a nuclear receptor gene, NR2E3, causes enhanced S cone syndrome, a disorder of retinal cell fate. *Nat Genet*. 2000;24:127–131.
9. Haider NB, Naggert JK, Nishina PM. Excess cone cell proliferation due to lack of a functional NR2E3 causes retinal dysplasia and degeneration in rd7/rd7 mice. *Hum Mol Genet*. 2001;10:1619–1626.
10. Milam AH, Rose L, Cideciyan AV, et al. The nuclear receptor NR2E3 plays a role in human retinal photoreceptor differentiation and degeneration. *Proc Natl Acad Sci USA*. 2002;99:473–478.
11. Roderick TH, Chang B, Hawes NL, Heckenlively JR. A new dominant retinal degeneration (Rd4) associated with a chromosomal inversion in the mouse. *Genomics*. 1997;42:393–396.
12. Nusinowitz S, Nguyen L, Radu R, Kashani Z, Farber D, Danciger M. Electroretinographic evidence for altered phototransduction gain and slowed recovery from photobleaches in albino mice with a MET450 variant in RPE65. *Exp Eye Res*. 2003;77:627–638.
13. Kitamura E, Kuemerle BA, Chernova OB, Cowell JK. Molecular characterization of the breakpoint region associated with a constitutional t(2;15)(q34;q26) in a patient with multiple myeloma. *Cancer Genet Cytogenet*. 2001;129:112–119.
14. Laemmli UK. Cleavage of structural proteins during the assembly of the head of bacteriophage T4. *Nature*. 1970;227:680–685.
15. Li X, Bachmanov AA, Li S, et al. Genetic, physical, and comparative map of the subtelomeric region of mouse Chromosome 4. *Mamm Genome*. 2002;13:5–19.
16. Lamb JC, Birchler JA. The role of DNA sequence in centromere formation. *Genome Biol*. 2003;4:214.
17. Horz W, Altenburger W. Nucleotide sequence of mouse satellite DNA. *Nucleic Acids Res*. 1981;9:683–696.
18. Manuelidis L. Consensus sequence of mouse satellite DNA indicates it is derived from tandem 116 basepair repeats. *FEBS Lett*. 1981;129:25–28.
19. Wong AK, Rattner JB. Sequence organization and cytological localization of the minor satellite of mouse. *Nucleic Acids Res*. 1988;16:11645–11661.
20. Kitanaka J, Wang XB, Kitanaka N, Hembree CM, Uhl GR. Genomic organization of the murine G protein beta subunit genes and related processed pseudogenes. *DNA Seq*. 2001;12:345–354.
21. Wang JC, Mamunes P, Kou SY, Schmidt J, Mao R, Hsu WT. Centromeric DNA break in a 10;16 reciprocal translocation associated

Downloaded from iovs.arvojournals.org on 08/16/2022

with trisomy 16 confined placental mosaicism and maternal uniparental disomy for chromosome 16. *Am J Med Genet*. 1998;80:418–422.

22. Tumer Z, Berg A, Mikkelsen M. Analysis of a whole arm translocation between chromosomes 18 and 20 using fluorescence in situ hybridization: detection of a break in the centromeric alpha-satellite sequences. *Hum Genet*. 1995;95:299–302.
23. Cantu ES, Khan TA, Pai GS. Fluorescence in situ hybridization (FISH) of a whole-arm translocation involving chromosomes 18 and 20 with alpha-satellite DNA probes: detection of a centromeric DNA break? *Am J Med Genet*. 1992;44:340–344.
24. Keen TJ, Mohamed MD, McKibbin M, et al. Identification of a locus (LCA9) for Leber's congenital amaurosis on chromosome 1p36. *Eur J Hum Genet*. 2003;11:420–423.
25. Kleinjan DJ, van Heyningen V. Position effect in human genetic disease. *Hum Mol Genet*. 1998;7:1611–1618.
26. Fantes J, Redeker B, Breen M, et al. Aniridia-associated cytogenetic rearrangements suggest that a position effect may cause the mutant phenotype. *Hum Mol Genet*. 1995;4:415–422.
27. Calvert PD, Krasnoperova NV, Lyubarsky AL, et al. Phototransduction in transgenic mice after targeted deletion of the rod transducin alpha-subunit. *Proc Natl Acad Sci USA*. 2000;97:13913–13918.
28. Humphries MM, Rancourt D, Farrar GJ, et al. Retinopathy induced in mice by targeted disruption of the rhodopsin gene. *Nat Genet*. 1997;15:216–219.
29. Lem J, Krasnoperova NV, Calvert PD, et al. Morphological, physiological, and biochemical changes in rhodopsin knockout mice. *Proc Natl Acad Sci USA*. 1999;96:736–741.

Downloaded from iovs.arvojournals.org on 08/16/2022